Numerical Simulation of Excess Ethanol Evaporation from Biodiesel in a Micro Heat-Exchanger

João L. Silva Jr.[a], Harrson S. Santana*[b], Geovanni B. Sanchez[b], Osvaldir P. Taranto[b]

[a]Federal Institute of Education, Science and Technology of South of Minas Gerais, 37550-000, Pouso Alegre, MG, Brazil.
[b]Faculty of Chemical Engineering, University of Campinas, 13083-852, Campinas, SP, Brazil.
harrison.santana@gmail.com

The transesterification is the most common method to produce biodiesel, usually, occurring with alcohol excess in order to displace the chemical reaction equilibrium to the products direction. After the reaction, this alcohol excess can be removed and recovered. In micro and macroscales, this procedure commonly takes place in evaporators or even in distillation columns. Hence, the present paper applied numerical simulation techniques to evaluate the excess alcohol separation from biodiesel in a microchannel heat-exchanger. Three process variables were investigated: temperature (80-120 ºC), flow rate (0.1-1.2 mL/min) and ethanol/biodiesel molar ratio, E:B (2-11). The results showed that an increase in the flow rate and molar ratio variables decreases the evaporation performance, in contrast with the positive effect of temperature (i.e., the increment of temperature provided an increase in the process). The use of micro heat-exchangers to perform the excess alcohol separation from biodiesel was numerically demonstrated.

1. Introduction

Aided by microfluidic tools, researchers have related several advantages in microscale biodiesel synthesis relative to conventional processes, especially in regard to the short residence times to reach high conversion levels (Rahimi et al., 2014). The transesterification of vegetable oils (chemical reaction between oil and methyl or ethyl alcohol in the presence of catalyst), normally occurs with excess alcohol, in order to displace the chemical reaction equilibrium to the products direction. After the reaction, the residual alcohol could be removed and recovered by evaporation. In macroscale, this procedure is commonly performed in evaporators or distillation columns. Recently, also at microscale level, researchers have been concentrated in biodiesel synthesis using microreactors, performing the product purification in conventional macroscale devices.

The evaporation process involves the heat transfer to the product stream followed by the phase change of the excess alcohol from liquid to vapor state. This phase change requires a great amount of heat added at a constant temperature (McCabe et al., 2001). Micro heat-exchangers could efficiently execute this process, due to its good superficial area-to-volume ratio and high heat flux. However, the evaporation in micro and milichannels, as well, the associate phenomena of heat and mass transfer are still not entirely understood due to the inherent complexity, and thus, detailed studies are essential (Zhang and Jia, 2016). In this context, the present research aims to present a mathematical model approaching the microdevice fluid dynamic, considering the heat and mass transfer phenomena, studying the effects of three fundamental operating variables: temperature, ethanol/biodiesel molar ratio and volumetric flow rate, in the excess alcohol evaporation process performance.

2. Mathematical Modeling

The mathematical model used was based on Volume of Fluid (VOF) approach. Three phases were considered: biodiesel, liquid ethanol and vapor ethanol. The mass (Equation 1) and energy (Equation 2) balances were solved for each phase, considering steady-state conditions:

$$\nabla \cdot \left(\alpha_k \rho_k U_k \right) = S_{m,k} \tag{1}$$

where the subscript k indicates the k-th phase (k = ve, le, b stand for ethanol vapor, ethanol liquid and biodiesel), α is the volumetric fraction of the phase, ρ is the specific mass (kg m^{-3}), U is the velocity vector (m s^{-1}), $S_{m,k}$ represents possible mass sources (kg m^{-3} s^{-1}). The biodiesel evaporation was neglected based on the biodiesel saturation temperature (340 °C – 375 °C, Goodrum, 2002), since it is well above the highest evaluated operating temperature of 120 °C. Therefore, the mass sources considered were: $S_{m,ve} = m_{vap}$, $S_{m,le} = - m_{vap}$, $S_{m,b} = 0$, where m_{vap} is the ethanol evaporation rate (kg m^{-3} s^{-1}), modeled in accordance with Equation 7.

$$\nabla \cdot \left(\alpha_k \rho_k U_k H_k \right) = \nabla \cdot \left(\alpha_k \lambda_k \nabla T_k \right) + S_{h,k} \tag{2}$$

where H is the specific enthalpy (J kg^{-1}), λ is the thermal conductivity (W m^{-1} K^{-1}), T is the thermodynamic temperature (K), S_h represents extra sources of interfacial heat transfer: $S_{h,le} = (Q_{le-ve} + Q_{le-b})$; $S_{h,ve} = - (Q_{b-ve} + Q_{le-ve})$; $S_{h,b} = (Q_{b-ve} - Q_{le-b})$, where Q_{k-i} indicates the heat rate transfer due to interphase convection, modeled by Equation 3:

$$Q_{k-i} = h_{k-i} a_{k-i} \left(T_i - T_k \right) \tag{3}$$

where k-i denotes the interaction between k-th and i-th phases, h_{k-i} is the convective heat transfer coefficient (W m^{-2} K^{-1}) and a_{k-i} is the specific interfacial area between the k-th and i-th phases (m^{-1}), given by Equation 4:

$$a_{k-i} = \frac{2|\nabla \alpha_k||\nabla \alpha_i|}{|\nabla \alpha_k| + |\nabla \alpha_i|} \tag{4}$$

The convective heat transfer coefficients, h, were estimated by Nusselt number, Nu, and phase properties, based on the empirical correlation for microchannels given by Kalaivanan and Rathnasamy (2011) (Equation 5):

$$Nu = \frac{hD_h}{\lambda} = 0.949 \, Re^{0.06} \, Pr^{0.4} \tag{5}$$

where D_h is the hydraulic diameter of the microchannels (m). The velocity and pressure fields where shared by the three phases, namely, a homogeneous modeling was used in the solution of momentum balance. This approach is recommended for VOF simulations, promoting superior numerical solution convergence. For multiphase flows at steady-state conditions, the homogeneous modeling provides:

$$\nabla \cdot \left(\rho U U \right) = -\nabla P + \mu \nabla^2 U + \rho g \quad \text{with} \quad \rho = \sum_{k=1}^{n_p} \alpha_k \rho_k \quad \text{and} \quad \mu = \sum_{k=1}^{n_p} \alpha_k \mu_k \tag{6}$$

where P is the pressure, μ is the dynamic viscosity (kg m^{-1} s^{-1}) and g is the gravity acceleration (m s^{-2}). The fluid properties, ρ and μ, were weighted by the volumetric fraction of each individual phase. The evaporation model employed was based on Phase Change Model by Saturation Temperature, available in the Ansys CFX (Rahmat and Hubert, 2010), as described in Equation 7:

$$m_{vap} = \left(\frac{h_{le}\left(T_{sat} - T_{le} \right) + h_{ve}\left(T_{sat} - T_{ve} \right)}{-H_v} a_{le-ve} \right) \quad \text{with} \quad H_v = 1.254 \times 10^6 \left(1 - \frac{T_{le}}{514} \right)^{0.31245} \tag{7}$$

where h is the convective heat transfer coefficient (W m^{-2} K^{-1}), a_{el-ev} is the ethanol liquid-vapor specific area (m^{-1}) (Equation 4), H_v is the evaporation specific enthalpy (J kg^{-1}), obtained from Poling et al. (2008), T_{sat} is the ethanol saturation temperature (78.4 °C), T_{le} and T_{ve} are the absolute temperature of liquid and vapor ethanol (K). The physical properties of ethanol were defined according to the operating temperature, estimated from expression given by Poling et al. (2008). The biodiesel physical properties were taken from literature (Esteban et al., 2012; Fasina et al., 2008).

3. Micro Heat-Exchanger Geometry and Simulation Conditions

The micro heat-exchanger used (Figure 1) consists in a microdevice of height of 210 μm, with one inlet, from where the mixture composed by liquid ethanol and biodiesel was introduced. The microdevice has 10 channels with a width of 500 μm, and two outlets: superior (vaporized ethanol outlet) and inferior (residual liquid ethanol and biodiesel outlet). The micro heat-exchanger geometry was created using the software

Autodesk Inventor 2015. The discretization process was carried out using the Ansys ICEM 14, resulting in about 255,000 tetrahedral control volumes (Figure 1(b-d)). The Ansys CFX 16 was used in the pre-processing, solver and post-processing steps. Steady-state simulations were performed. High resolution interpolation schemes were employed, and the number of iterations was defined between 100 and 1000, with the root mean square residual target of 10^{-4}.
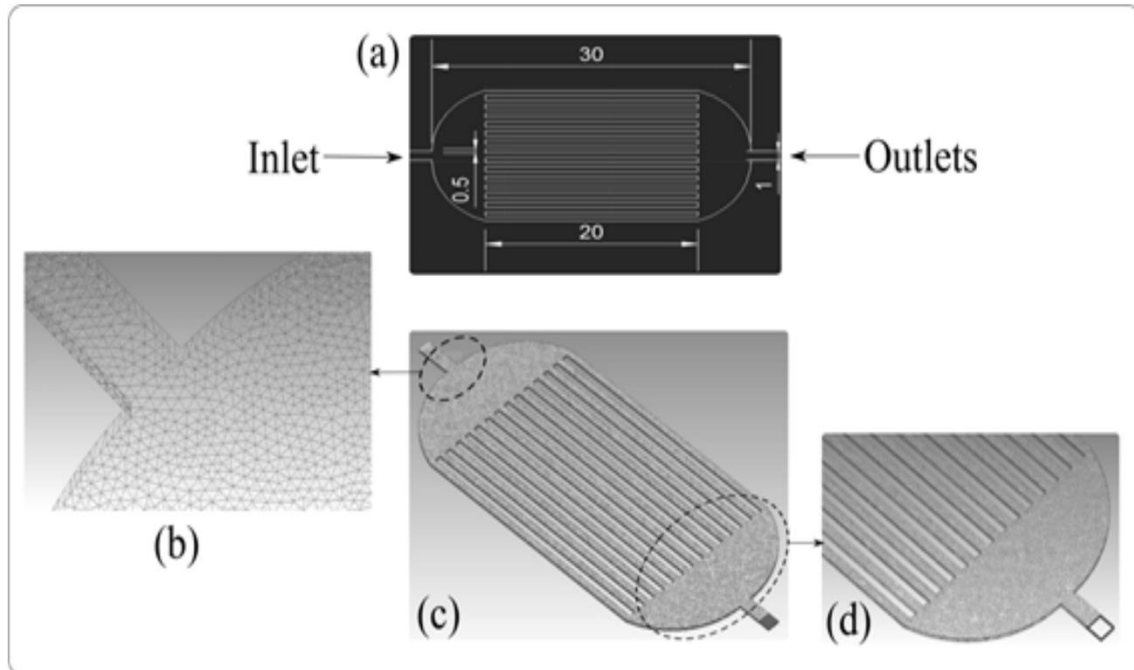

Figure 1: (a) Micro heat-exchanger geometry with dimensions in milimeters; Numerical mesh details: (b) entrance region; (c) microdevice; (d) outlet region.

A Central Composite Rotatable Design (CCRD - 2^3) was employed to analyse the effects of three operating variables on ethanol evaporation performance: temperature (80-120 °C), mixture volumetric flow rate (0.1-1.2 mL/min), ethanol/biodiesel molar ratio, E:B (2-11). The evaporation process performance was evaluated using the Vaporized Ethanol Percentage - VEP (%), given as the ratio of mass flow rate of vapor ethanol at superior outlet by the mass flow rate of liquid ethanol entering the microdevice, according to Equation 8:

$$VEP(\%) = 100 \cdot \left(\frac{\dot{m}_{ve,outlet\ vapor}}{\dot{m}_{le,inlet}} \right)$$

(8)

The employed boundary conditions were:
- Inlet: velocity, temperature and compound fractions prescribed in accordance with the case;
- Outlets: opening to relative pressure zero, prescribed temperature in accordance with the case;
- Heat Plate and Walls: no-slip boundary conditions for all phases, prescribed temperature in accordance with the case.

4. Results and Discussion

The evaporation performance was evaluated using a Central Composite Rotatable Design (CCRD), analysing the effect of three operating variables (temperature, mixture flow rate, ethanol/biodiesel molar ratio), using six axial points and one central point, resulting in 15 runs. Table 1 presents the VEP (%) predictions. For the studied conditions, VEP (%) ranged from 6.90% to 63.74%. Using the simulation results, the effects of each one of the three process variables in the evaporation performance were calculated using the software Statistica 7, as summarized in Table 2. Considering a statistical significance level of 95% (p-value < 0.05), the linear terms of temperature (x_1), flow rate (x_2) and E:B molar ratio (x_3) were statistically significant. Accordingly, the numerical predictions showed that the evaporation efficiency (vaporization of ethanol liquid molecules to vapor state) is strongly affected by the evaluated process variables. The increment of

temperature provided an increase in the vaporized ethanol percentage, while the decrease of both, flow rate and E:B molar ratio, resulted in higher evaporation efficiencies. This behavior is illustrated in the Pareto diagram (Figure 2). Figure 3 shows the good agreement by the mathematical model in data prediction, explaining 94.97% of data variability.

Table 1: Description of operating conditions and VEP(%) results for the cases of study.

Case	Q (mL/min)	T (ºC)	E:B Molar Ratio	VEP(%)
1	0.3	88	4	32.79
2	0.3	112	4	58.59
3	0.9	88	4	16.56
4	0.9	112	4	36.23
5	0.3	88	9	25.32
6	0.3	112	9	45.19
7	0.9	88	9	25.31
8	0.9	112	9	27.40
9	0.6	80	6.5	6.90
10	0.6	120	6.5	39.71
11	0.1	100	6.5	63.74
12	1.2	100	6.5	21.71
13	0.6	100	2	46.54
14	0.6	100	11	25.95
15	0.6	100	6.5	30.39

Table 2: Variables effects on vaporized ethanol percentage, VEP (%).

| Factor	Effects	Std. Deviation	t(5)	p-value	Interval Estimative (95%)	
					Inferior Limit	Superior Limit
Average	30.56	5.69	5.36	0.003	15.91	45.21
x_1 (L)	17.96	3.10	5.79	0.002	9.98	25.93
x_1 (Q)	-5.48	4.66	-1.17	0.292	-17.46	6.49
x_2 (L)	-18.61	3.10	-5.99	0.002	-26.58	-10.64
x_2 (Q)	8.24	4.66	1.77	0.137	-3.73	20.22
x_3 (L)	-8.13	3.10	-2.62	0.047	-16.11	-0.17
x_3 (Q)	3.66	4.66	0.77	0.467	-8.31	15.64
x_1x_2	-5.98	4.05	-1.47	0.200	-16.39	4.44
x_1x_3	-5.88	4.05	-1.45	0.207	-16.29	4.54
x_2x_3	5.19	4.05	1.28	0.256	-5.22	15.61

% explained variation (R^2) = 94.97
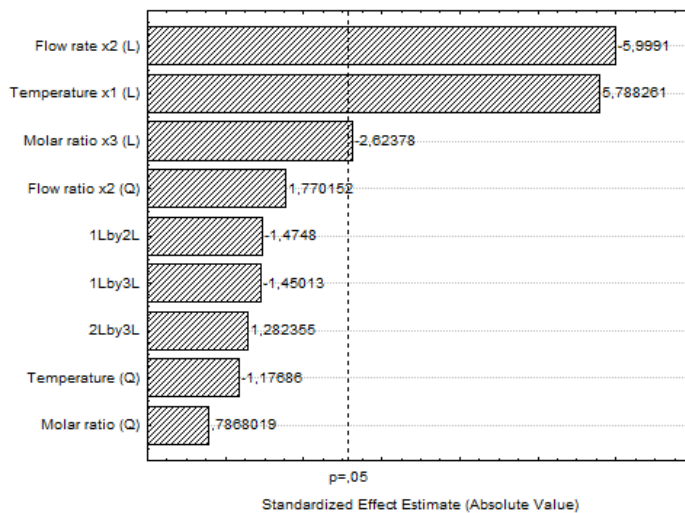
Figure 2: Pareto diagram for the operating variables effects on vaporized ethanol percentage, VEP (%).
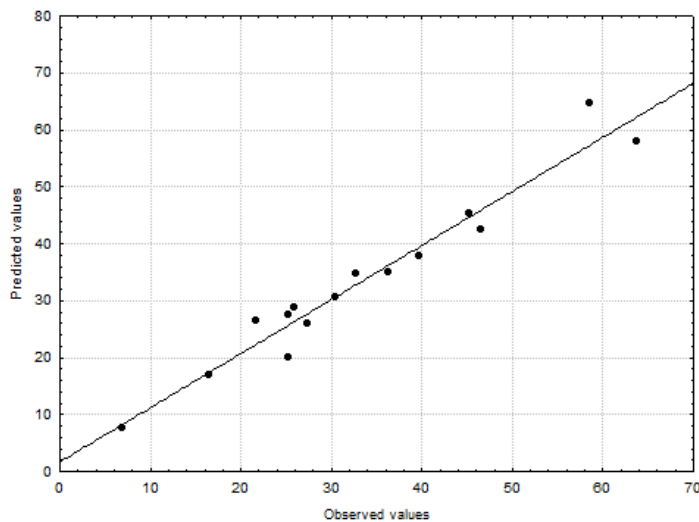

Figure 3: Observed and predicted values for vaporized ethanol percentage, VEP (%).

The temperature influence on ethanol evaporation can be analyzed by the relation between vaporized mass and heat of vaporization ($m = Q \, H_v^{-1}$), where an inverse relationship between the mass and the energy amount is observed. In Equation 7, the increment of temperature promotes a decrease in the heat of vaporization, and thus, increasing the vaporized mass.

The flow rate effect also could be explained by the relationship between vaporized mass and heat of vaporization. The increment of flow rate results in a decrease of fluid residence time inside the micro heat-exchanger, resulting in lower rates of heat received by the fluid mixture, consequently, influencing the ethanol evaporation rate.

The ethanol/biodiesel molar ratio yielded negative influence in ethanol evaporation performance, namely, the increment of E:B molar ratio decrease the *VEP* (%). This behavior could be related to the heat transfer phenomena between the liquid phases (ethanol and biodiesel). When a smaller amount of biodiesel is present, the liquid ethanol received lower amounts of heat, resulting in reduced vaporized ethanol percentages. Analyzing the predicted averaged values of interfacial heat transfer rate between liquid ethanol and biodiesel ($S_{h,el} = Q_{el-ev} + Q_{el-b}$) for the cases 13 (E:B molar ratio = 2), 15 (E:B molar ratio = 6.5) and 14 (E:B molar ratio = 11), the results were respectively, 1.26×10^{-7} W m^{-3}, -6.22×10^{-6} W m^{-3} and -5.25×10^{-6} W m^{-3}, substantiating this justification.

5. Conclusions

In the present research a mathematical model approaching the fluid dynamics coupled with heat and mass transfer due to evaporation in microdevices was presented. The effect of three operation variables (temperature, mixture flow rate and ethanol/biodiesel molar ratio) on the ethanol evaporation performance was numerically studied. The temperature influenced positively the evaporation performance, since it is directly related to the thermal energy transferred to the fluid flow. The ethanol/biodiesel molar ratio and the flow rate affected negatively the evaporation process. The latter one, due to the residence time of the liquid mixture required to the evaporation of liquid ethanol. The effect of E:B molar ratio was related to the real heat amount available in the liquid ethanol, due to the liquid ethanol-biodiesel interfacial convective heat transfer phenomena, where smaller relative amounts of biodiesel provided greater interfacial heat transfer rates, resulting in superior evaporation performance. In summary, the application of micro heat-exchangers in the ethanol evaporation from biodiesel mixtures was numerically demonstrated.

Acknowledgments

Reference

Caney, N., Louahlia-Gualous, H., Bontemps, A., 2016, Two-Phase Flow in Microchannels. In: Microscale and Nanoscale Heat Transfer: Analysis, Design and Applications, CRC Press, 2016.

Esteban, B., Riba, J.R., Baquero, G., Rius, A., Puig, R., 2012, Temperature dependence of density and viscosity of vegetable oils. Biomass and Bioenergy, 42, 164-171.

Fasina, O.O., Colley, Z., 2008. Viscosity and specific heat of vegetable oils as a function of temperature: 35 °C to 180 °C. International Journal of Food Properties, 11, 738-746.

Goodrum, J.W., 2002, Volatility and boiling points of biodiesel from vegetable oils and tallow. Biomass and Bioenergy, 22, 3, 205-211.

Kalaivanan, R., Rathnasamy, R., 2011, Experimental Investigation of Forced Convective Heat Transfer in Rectangular Micro-channels, Jordan Journal of Mechanical and Industrial Engineering, 5, 383-387.

Lineykin, S., Ben-Yaakov, S., 2007, Modeling and Analysis of Thermoelectric Modules, IEEE Transactions on industry application, 43, 505-515.

McCabe, W.L., Smith, J.C., Harriott, P., 2005, Unit operation of Chemical Engineering, 7th edition, McGraw-Hill, New York, USA.

Poling, B.E., Thomson, G.H., Friend, D.G., Rowley, R.L., Wilding, W.V., 2008, Physical and Chemical Data. In: Perry's Handbook of Chemical Engineering, 8th. Edition, McGraw-Hill Education, New York, USA.

Rahimi, M., Aghel, B., Alitabar, M., Sepahvand, A., Ghasempour, H.R., 2014, Optimization of biodiesel production from soybean oil in a microreactor, Energy Conversion and Management, 79, 599-605.

Rahmat, M.; Hubert, P., 2010, Two-phase simulations of micro heat pipes, Computers & Fluids, 39, 451-460.

Zhang, P., Jia, H.W., 2016, Evolution of flow patterns and the associated heat and mass transfer characteristics during flow boiling in mini-/micro-channels, Chemical Engineering Journal, 306, 978-991.